Nuclear Instruments and Methods 208 (1983) 489–494
North-Holland Publishing Company

SMALL ANGLE X-RAY SCATTERING STUDY OF PHASE SEPARATION IN GLASSES USING A NEW POSITION SENSITIVE DETECTOR

Serge BRAS
Elphyse, Yerres, France

Aldo CRAIEVICH *
L.U.R.E., Universite Paris-Sud, Orsay, France

Juan M. SANCHEZ
Henry Krumb School of Mines, Columbia University, New York, USA

Claudine WILLIAMS
College de France, Paris, France and L.U.R.E.–Universite Paris-Sud, Orsay, France

Edgar D. ZANOTTO
Universidade Federal de Sao Carlos, Sao Carlos, Brazil

A recent study by small angle X-ray scattering (SAXS) of phase separation in a borate glass agreed with the predictions of statistical theories for the demixing process. Here, additional data on the B_2O_3–PbO–Al_2O_3 system, obtained with synchrontron radiation, are reported. The heat treatment of the sample is performed in situ and the SAXS intensities are measured using a new one-dimensional position sensitive detector. Experimental SAXS data have been collected for different durations of isothermic treatment, in the middle and near the boundary of the miscibility gap. The data suggest the general validity of the dynamical scaling hypothesis of the statistical theory of phase separation in glass systems.

1. Introduction

The first theoretical study of the complex phenomena of phase separation in solid mixtures was provided by the now classic theory of spinodal decomposition of Cahn [1]. Central to the theory is the fact that, within the so-called spinodal region, the homogeneous mixture is unstable to small concentration fluctuations. Cahn was able to derive an equation for the time evolution of such fluctuations, from which the evolution of the X-ray scattering at small angles followed directly. Unfortunately, the evolution equation for the scattered intensity could only be solved in closed form after linearization and, therefore, the theory is in principle only applicable to the very early stages of decomposition.

Outside the spinodal region, i.e. near the boundaries of the miscibility gap, the decomposition process was described by the classical diffusion theories of nucleation and growth of "zones" (in alloys) or "droplets" (in glasses).

The fact that two seemingly unrelated theories were needed to describe the decomposition process strongly suggested that one should be able to experimentally distinguish the "spinodal" and the "nucleation and growth" regions in the miscibility gap. The boundary between these two regions being given by the spinodal curve. Thus, the early experimental effort was directed towards the verification of Cahn's theory for very short decomposition times and to the location of the spinodal curve.

The views that only the early stages were amenable to detail analysis and that a sharp change in mechanism should be observed at both sides of the spinodal have been, of course, greatly dispelled by more recent theoretical work.

A clear indication that the boundary between the "spinodal" and the "nucleation and growth" regions was blurry, so to speak, was the introduction of fluctuation terms and non-linearities in the evolution equation, both missing in Cahn's original treatment. For an early

* Present address: Centro Brasileiro de Pesquisas Fisicas, Rio de Janeiro, Brazil.

0167-5087/83/0000–0000/$03.00

treatment of the non-linear theory of spinodal decomposition, the reader is referred to work of Langer [2].

More recent developments have considerably simplified the picture of the decomposition process at later times. In particular, Monte Carlo simulations by Marro, Lebowitz and Kalos [3], seem to suggest simple scaling properties for the time dependent structure function of isotropic systems. The computer simulation results also indicate that the scaling properties hold throughout the miscibility gap, without distinction between the spinodal and the nucleation and growth regions.

Measurements of small angle X-ray scattering in glasses stand out as an invaluable tool for the scrutiny of existing theories since the technique gives direct access to the structure function of an isotropic mixture. In fact, recent experimental work [4] using small angle X-ray scattering in a B_2O_3–PbO–Al_2O_3 glass within the spinodal region, suggested that the dynamical scaling hypothesis is valid for this system. In order to test the general applicability of the scaling hypothesis, we present here a comparative study of the glass system investigated in ref. 4 with another whose composition and temperature puts it within the "nucleation and growth" region of the miscibility gap.

In a previous work [4], two of the present authors emphasized the interest of performing additional experiments on glasses using more favorable experimental conditions than those available in conventional X-ray laboratories. Here we present new scattering data obtained with a synchrotron radiation source and a new position sensitive detector.

2. Experimental

Reagent grade H_3BO_3, PbO and Al_2O_3 were used to obtain 80 B_2O_3–15 PbO–5 Al_2O_3 and 64 B_2O_3–27 PbO–9 Al_2O_3 (wt%) glasses. Each batch was melted in a platinum crucible and homogenized at 1200°C by stirring for several hours. The melts were quenched by the splat-cooling technique. The resulting thin glass platelets had the appropriate thickness for the small angle X-ray scattering studies and thus, required no further treatment.

The synchrotron radiation beam at LURE was monochromatized by a bent germanium crystal [5]. The bent crystal and the use of appropriate slits provided a beam of wavelength $\lambda = 1.38$ Å with pin-hole collimation. The glass samples were held at constant temperature during the scattering measurements by means of a high temperature cell [6]. A one-dimensional position sensitive detector of slit width 1 mm was placed at 1 m from the sample. The time interval during which scattered intensity was allowed to accumulate was kept much shorter than the time between each measurement.

3. X-ray detector

A schematic drawing of the detector is shown in fig. 1. The main body of the detector is a sealed, gas-filled counter with a wide entrance slit s. The electrode within the gas-filled volume consist of a metallic cathode coil k wound around a straight thin anode wire a. A high voltage, typically 1800 V, is applied between both electrodes. The position of the avalanche of secondary electrons produced by each absorbed photon is determined from the signal induced in the 15 μm thick wire of the cathode coil. A significant advantage of the present cathode geometry over that of conventional position sensitive detectors is the stronger signal induced by the avalanche. Since the diameter of the cathode wire is a small fraction of the coil pitch, the loss of photons due to absorption in the cathode is negligible.

The signals arriving at the ends of the cathode are used to localize the incoming photon. The signal collected on the anode wire is used for energy discrimination. The electronic treatment of the signals is the classical double differentiation at each end of the cathode. The position of the incoming photon is a function of the difference between the zero cross-over time of both signals.

The detector gas is a 90% argon–10% methane mixture. The resolution of the detector can be seen in fig. 2a, where the multichannel analyzer spectra with a 50 μm slit are represented for three counting rates. The width of the peak is 150 μm at low counting rates and increases to 170 μm at high counting rates. The linearity was determined from the spectrum shown in fig. 2b which was obtained with fixed slit by moving the detector by 5 mm steps. The linearity was found to be better than 1% over 45 mm.

The uniformity of the efficiency for 8 keV photons is $\pm 2\%$ over 45 mm and the resolution in energy is

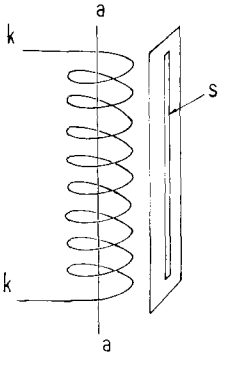

Fig. 1. Schematic detector geometry. The straight wire a is the anode, the coil k the cathode and s the entrance slit.

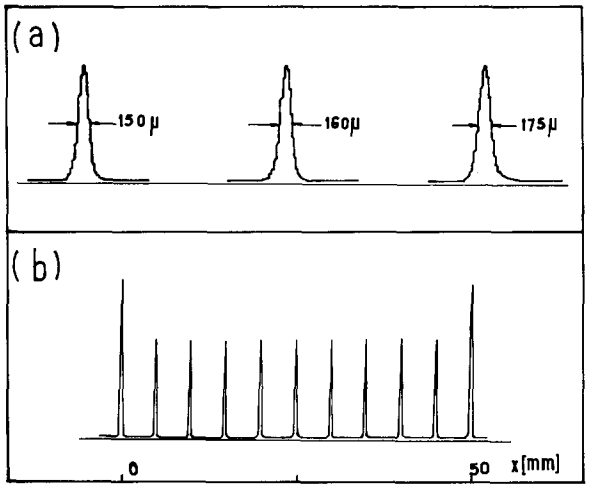

Fig. 2. (a) Multichannel analyzer profile of a 50μ slit at different counting rates: 3000 c/s (left), 15000 c/s (center) and 40000 c/s (right). (b) Multichannel analyzer spectrum of a fixed slit obtained by moving the detector by 5 mm steps.

between 15 and 20% depending on the experimental conditions. The maximal counting rate is between 30 and 40000 counts per second, depending on the spatial distribution of the photons.

4. Results and discussion

Small angle X-ray scattering data were obtained for 80 B_2O_3–15 PbO–5 Al_2O_3 and 64 B_2O_3–27 PbO–9 Al_2O_3 glasses, held at 460 and 490°C, respectively. The resolution, linearity, homogeneity and maximal counting rate of the detector together with the pin-hole collimation of the X-ray beam, assured that the different sets of scattering curves are essentially free from instrumental aberrations.

The small angle scattering curves for the glasss system 80 B_2O_3–15 PbO–5 Al_2O_3 correspond to the spinodal region of the miscibility gap. The smoothed scattering curves are shown in fig. 3 for different times t as a function of the modulus of the scattering vector, defined by

$$q = 4\pi \sin \theta/\lambda,$$

where θ is half the scattering angle and λ is the X-ray wavelength. The set of scattering curves shows continous increase of the scattering intensity and shift of the maximum to lower values of q with increasing t.

The scattering curves from the glass 64 B_2O_3–27 PbO–9 Al_2O_3 are shown in fig. 4. This glass system is in the "nucleation and growth" region near the miscibility gap boundary. The same qualitative fea-

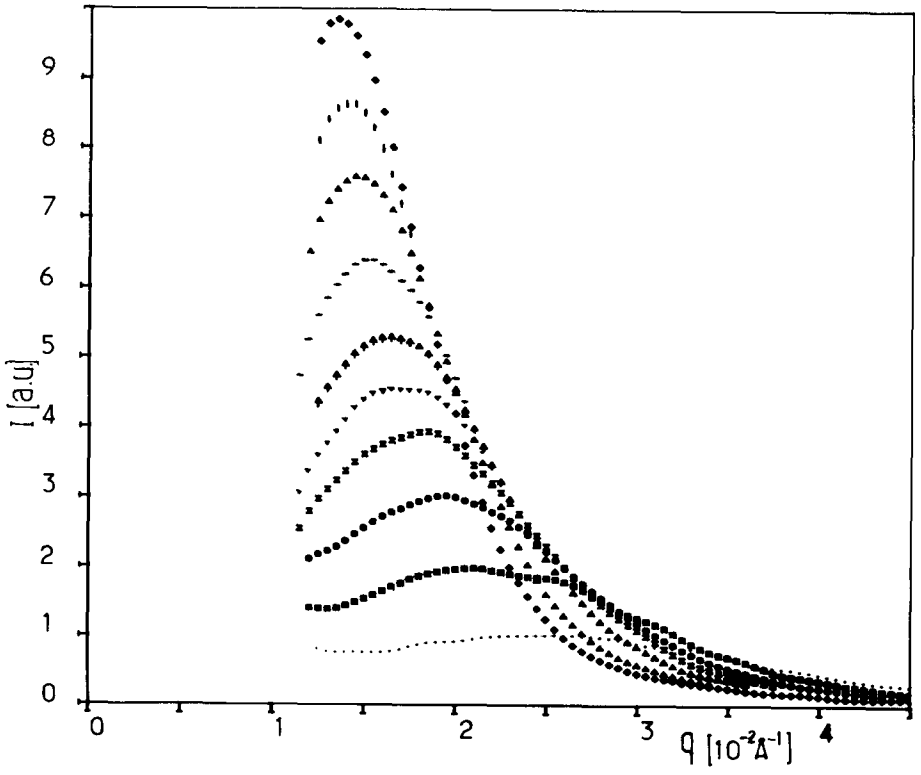

Fig. 3. Time evolution of the small angle X-ray scattering at 460°C for a 80 B_2O_3–15 PbO–5 Al_2O_3 glass. The times (min) are: • 3.7, ■ 10.0, ● 18.1, ⧗ 25.6, ▼ 31.1, ↑ 37.3, – 46.9, ▲ 57.0, | 67.2, ◆ 78.0.

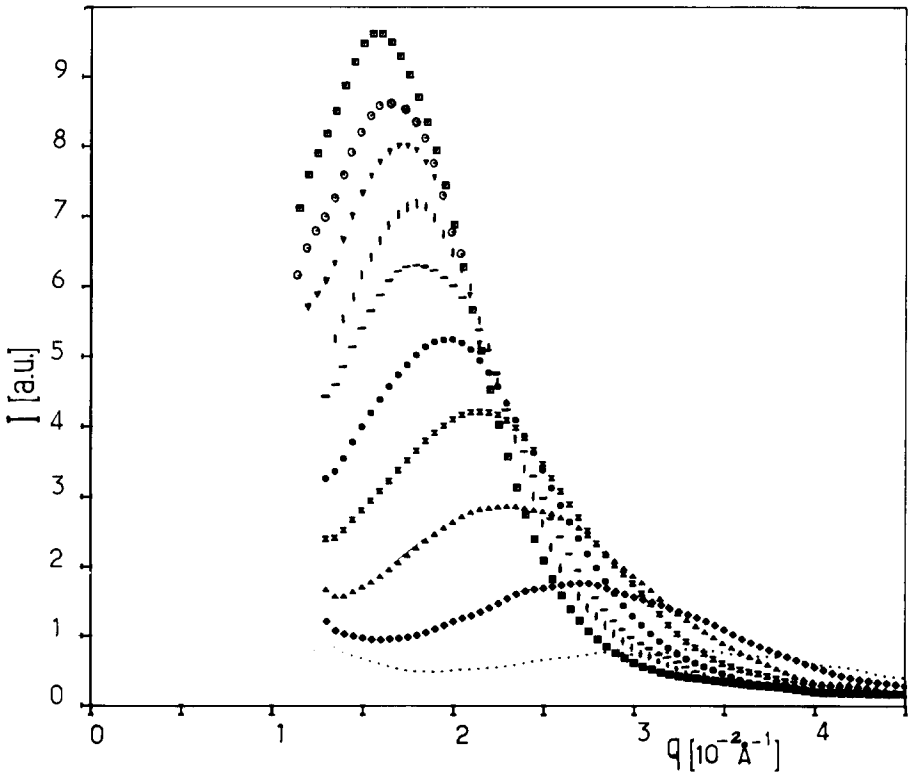

Fig. 4. Time evolution of the small angle X-ray scattering at 490°C for a 64 B_2O_3–27 PbO–9 Al_2O_3 glass. The times (min) are: • 5.0, ◆ 9.5, ▲ 16.0, ⧗ 23.0, ● 30.5, – 39.0, | 44.0, ▼ 50.5, ⊙ 56.5, ⊡ 65.0.

tures observed in the 80 B_2O_3–15 PbO–5 Al_2O_3 system are evident for this glass.

The test of validity of the scaling property was made on the sets of scattering curves of figs. 3 and 4. The scaling relation inferred from the Monte Carlo simulation [3] of the intensity scattered by isotropic systems in advanced stage of phase separation, can be written as:

$$I(q,t)\,q_m^3(t) = F(x), \tag{1}$$

where $q_m(t)$ is the q value corresponding to the maximum of the scattered intensity at a time t, $F(x)$ is a scaling function and x is equal to $q/q_m(t)$. The function $q_m(t)$ varies with time according to a power law:

$$q_m(t) \propto t^{-a}. \tag{2}$$

According to the computer simulations the exponent a increases from 0.20 near the center to 0.28 near the boundary of the miscibility gap.

The q_m values for the intensity curves of figs. 3 and 4 were determined by a parabolic fitting of the smoothed curves. The scaling functions $F(x)$ corresponding to advanced stages of phase separation are presented in figs. 5 and 6 for the two compositions investigated. The different curves agree reasonably well with the scaling hypothesis of eq. (1). Nevertheless, discrepancies for some of the curves are apparent.

Another critical test of the theoretical models is the analysis of the validity of eq. (2). The plots of the q_m values as a function of time in double logarithmic scale, given in fig. 7, agree with the theoretical linear behavior. The exponent a obtained from fig. 7 is 0.24 for the 80 B_2O_3–15 PbO–5 Al_2O_3 glass, in agreement with previous experimental work [4] and with the computer simulation results [3]. The exponent a for the 64 B_2O_3–27 PbO–9 Al_2O_3 glass is found to be 0.28, in remarkable agreement with the theoretical prediction for systems near the boundaries of the miscibility gap [3].

Overall, our experimental results are in close agreement with recent Monte Carlo simulations [3] and, despite some discrepancies, they strongly suggest the validity of the scaling hypothesis throughout the miscibility gap. The observed deviations from the scaling hypothesis for some of the scattering curves remain unresolved at the present time. Such discrepancies may be due, however, to the intrinsic inaccuracy in determin-

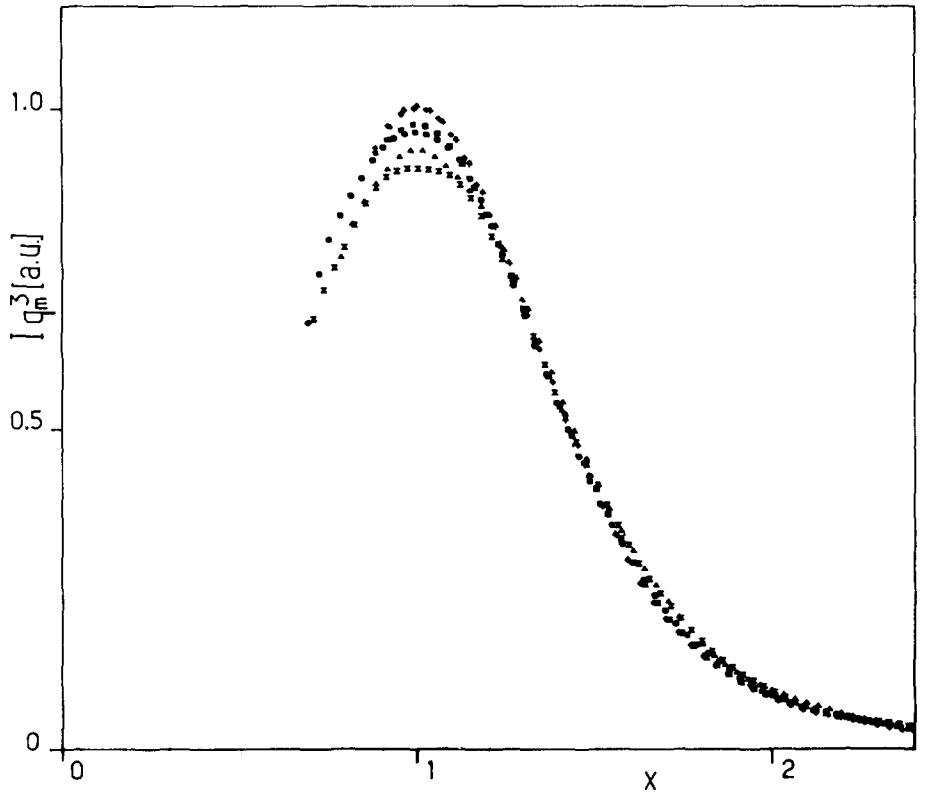

Fig. 5. Scaling of thfe scattering curves of fig. 3 for advanced stages of phase separation. The times (min) are: ⧗ 31.1, ● 37.3 , ▲ 46.9, ■ 57.0, ◆ 67.2, ↟ 78.0.

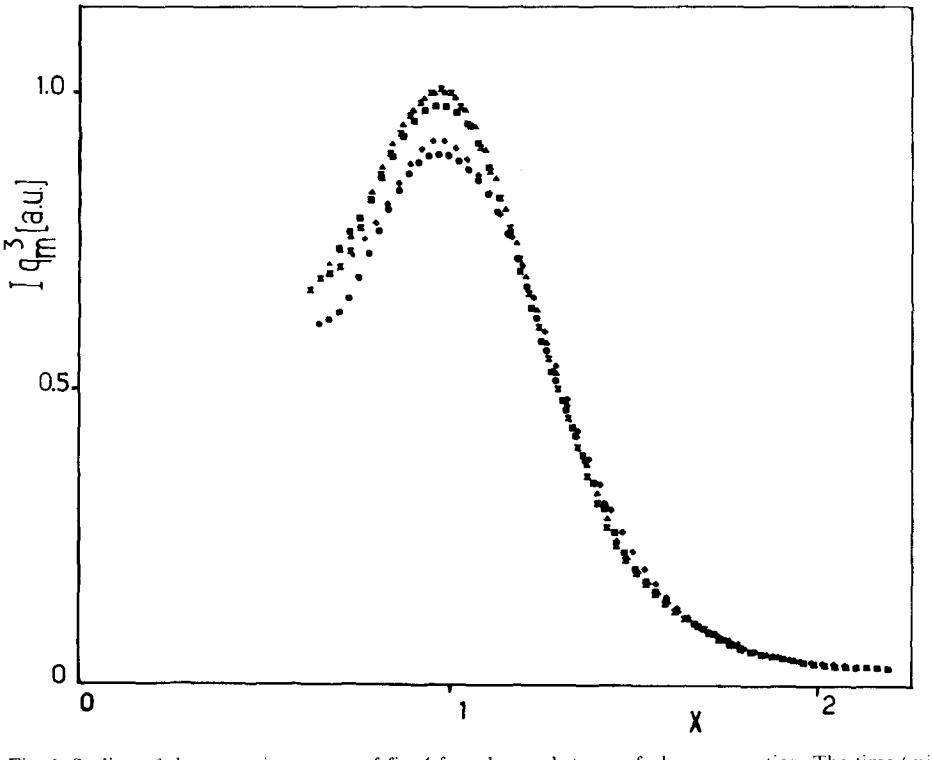

Fig. 6. Scaling of the scattering curves of fig. 4 for advanced stages of phase separation. The time (min) are: ● 39.0, ⧗ 44.0, ▲ 50.5, ■ 56.5, ◆ 65.0.

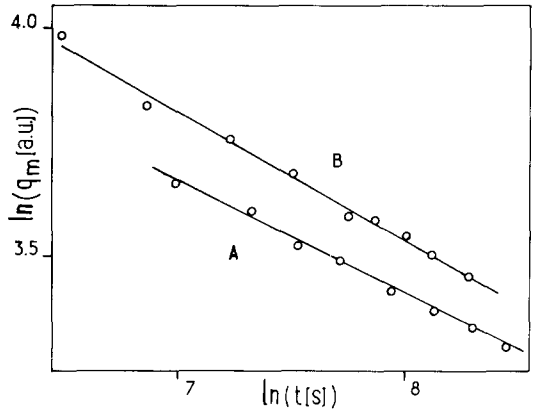

Fig. 7. Time dependence of $q_m(t)$ for glasses 80 B_2O_3–15 Al_2O_3 (A) and 64 B_2O_3–27 PbO–9 Al_2O_3 (B). The full lines correspond to exponents $a = 0.24$ (A) and $a = 0.28$ (B).

ing the position of the intensity maxima. A more precise test of the scaling hypothesis involving the several moments of the scattering curves and a similar analysis for results over a range of temperature are in progress.

5. Conclusions

The use of synchrotron radiation, a new position sensitive detector and a high temperature cell for in situ heat treatments, allowed us to obtain small-angle scattering data from glasses which can be compared directly with the predictions of the theories of time evolution for demixing processes.

The results presented show essentially the same general behavior of the scattered intensity for glass systems at the center and near the boundary of the miscibility gap. The dynamical scaling hypothesis was tested for the two systems investigated. The results of the analysis suggest the general validity of the Monte Carlo simulations and, particularly, of the dynamical scaling hypothesis in glasses. The experimental results are in support of the idea that a single mechanism is responsible for demixture over the whole miscibility gap, without the existence of a sharp separation between "spinodal" and "nucleation and growth" regions.

References

[1] J.W. Cahn, Trans. Metall. Soc. AIME 242 (1968) 166.
[2] J.S. Langer, Am. Phys. (N.Y.) 65 (1971) 53.
[3] J. Marro, J.L. Lebowitz and M.H. Kalos, Phys. Rev. Lett. 43 (1979) 282.
[4] A. Craievich and J.M. Sanchez, Phys. Rev. Lett. 47 (1981) 1308.
[5] D. Tchoubar, F. Rousseaux, C.H. Pons and M. Lemonnier, Nucl. Instr. and Meth. 152 (1978) 301.
[6] A. Craievich, J. Appl. Cryst. 7 (1974) 634.